General Relativity and Gravitation (2025) 57:133
https://doi.org/10.1007/s10714-025-03469-z

RESEARCH

The influence of a minimal length and accumulation of dark energy near the event horizon and the stability of a black hole

L. Maglahoui[1,2] · P. O. Hess[3,4]

Received: 23 May 2025 / Accepted: 17 September 2025

Abstract
We investigate the influence of a minimal length and the accumulation of dark energy on the structure of black holes, for Schwarzschild and Kerr solutions. We show that near the event horizon the minimal length creates a region of negative temperature, resulting in a negative pressure, which counteracts a collapse. When dark energy is added, in addition the position of the event horizon will change and, depending on the size of the dark energy, stable dark stars are created. Our study ranges from standard black holes (no minimal length and no dark energy) to black holes with a minimal length and various radial intensities for the accumulation of dark energy. The dependence of the effects as a function of the black holes's mass is studied. We find that a minimal length is possibly responsible for the suppression of primordial black holes.

Keywords General Relativity · psuedo-complex · General Relativity · minimal length · black holes

1 Introduction

Black holes (BH) are still the subject of numerous investigations. They represent extreme objects, predicted by General Relativity (GR): If a star is massive enough, within GR all matter falls into a singularity at the center of a BH. It also creates an event horizon at a certain distance from the center, marking a radial position below which

✉ P. O. Hess
hess@nucleares.unam.mx

1 Physics Department, University of Mentouri, Constantine 1 Constantine P. O. Box 325, Ain El Bey Way, 025017 Constantine, Algeria

2 Mathematical and Subatomic Physics Laboratory (LPMPS) University of Mentouri, Constantine, Algeria

3 Instituto de Ciencias Nucleares, UNAM, Circuito Exterior, C.U. A.P. 70-543, 04510 México, D.F., Mexico

4 Frankfurt Institute for Advanced Studies, J. W. von Goethe University, Hessen, Germany

Published online: 23 September 2025

not even light can escape. One can accept these consequences or not. A singularity at the center and also the formation of an event horizon are signatures that GR reached its limits and some information is missing. Even when event horizons are common in GR and have a natural explanation [1], the one of a BH is different, as it is a consequence of a very strong gravity. Extreme situations in a physical theory always raises the question, if that theory has to be modified. One such possibility is Quantum Gravity, a topic of intense research. Attempts to modify GR are numerous, we just refer to theories like Quantum Loop Gravity [2] and String Theory [3]. While the first supposes a discrete structure of space-time, the second introduces smallest elementary objects in form of strings. There has been a lot of efforts in recent decades to extract predictions from them, i.e., calculating consequences of these theories, with little success. Therefore, the question is if not effective theories, easier to apply, can help in these situations. And indeed, there are many attempts to extend and modify GR, as for example modified gravity models [4], mostly adding higher terms in the Ricci scalar R. In order to combine with a quantized description of GR, the Hořawa-Lifshitz quantum gravity [5] description was developed, which breaks Lorentz invariance at high energy by effectively introducing a minimal length. This model is combined with non-commuting variables in [6], also introducing in such a manner a minimal length. Apart of a minimal length, another effect is the presence of vacuum fluctuations, denoted as dark energy. As noted, for example, in [7] a curved space provokes vacuum fluctuations, which is also demonstrated in [8]. These vacuum fluctuations are repulsive and act against gravitation. The vacuum fluctuations, from now on called dark energy, increase toward lower distances to the BH and are singular (becoming infinite) at the event horizon. However, no back-reactions were taken into account, i.e., the infinite value has to be taken with a grain of salt. Another possibility is to model the increase of the dark energy density by B_n/r^n, as done in [9–11], within the so-called pseudo complex General Relativity (pcGR). This theory doubles the number of variables by introducing pseudo-complex variables, the only possible extension of coordinates which does not result in tachyon or ghost solutions [12]. Reducing through a constraint to a four-dimensional space [11] leads to the appearance of a dark energy term in the Einstein equations. The dark energy results to be anisotropic [13] and in practical applications the dark energy density is modelled by the above mentioned dependence in the radial distance. The pcGR can be reduced to many other models with a minimal length (maximal acceleration, see for example [14]), which we cannot mention here all and we refer to the reference list in [11]. The pcGR includes both, a minimal length and the presence of dark energy and it is, therefore, ideal to use for the purpose of this contribution. It allows to vary the contribution of dark energy from non-existent (GR) to any higher value, though there will be an upper limit for a representational purpose. It also contains a minimal length, which we can skip or not, i.e., we can determine the differences when a minimal length is taken into account and when not. Also interesting is the change of the effects of a minimal length as a function of the mass of the BH. We will introduce the parameter $\epsilon = l/m$, which ranges from 1 to very small values, which correspond to large mass BH. For large, macroscopic black holes, the question is if the effects of the minimal length are still present or disappear.

This paper is organized as follows: In Section 2 a short resumé is presented on how the dark energy and the minimal length arise in pcGR. In Section 3 the Kerr metric with

a dark energy contribution is listed and in a first subsection the discussion is restricted to the Schwarzschild solution (no rotation present). In a second, short subsection rotation is added (Kerr), but only the main differences to the Schwarzschild solution is outlined. In Section 4, Conclusions will be drawn.

Throughout the paper we use $G = c = 1$, where G is the gravitational constant. The metric signature is $(+ - --)$.

2 A model with dark energy and a minimal length

Let us extend algebraically the GR, which means to define other types of coordinates instead the real valued coordinates x^μ ($\mu = 0, 1, 2, 3$). One such coordinate type are the pseudo-complex variables

$$X^\mu = x^\mu + I y^\mu = X^\mu_+ \sigma_+ + X^\mu_- \sigma_- \tag{1}$$

with $I^2 = 1$ and $\sigma_\pm = \frac{1}{2}(1 \pm I)$. This introduces four real variables y^μ and, thus, increases the dimension of space-time from 4 to 8. The $\sigma_\pm$ satisfy the property $\sigma_\pm^2 = \sigma_\pm$ and $\sigma_+\sigma_- = 0$. Due to $I^2 = 1$ we call these variables pseudo-complex and hence its name. Due to the properties of the $\sigma_\pm$ operators, the pseudo-complex variables form a ring instead of a field. Furthermore, the components in σ_+ and σ_- are called zero-divisor components. It is important to note, already mentioned in the introduction, that only the pseudo-complex extension does not lead to tachyon and ghost solutions, all other coordinate extensions do [12].

In each sector $\sigma_\pm$ a metric can be defined, namely $g^\pm_{\mu\nu}$ and their symmetric and anti-symmetric combinations are, respectively,

$$g^S_{\mu\nu} = \frac{1}{2}(g^+_{\mu\nu} + g^-_{\mu\nu}),\ g^A_{\mu\nu} = \frac{1}{2}(g^+_{\mu\nu} - g^-_{\mu\nu}) \tag{2}$$

The action of this theory is of the same form as in GR, namely

$$S = \int d^4X \sqrt{-g}(R + 2\alpha) \tag{3}$$

with the distinction that all expressions appearing in (3) are now pseudo-complex, including the integral. With $g_{\mu\nu} = g^+_{\mu\nu}\sigma_+ + g^-_{\mu\nu}\sigma_-$, the length element is given by

$$\begin{aligned} d\omega^2 = g_{\mu\nu} dX^\mu dX^\nu = &\left\{ g^S_{\mu\nu}[dx^\mu dx^\nu + dy^\mu dy^\nu] + g^A_{\mu\nu}[dx^\mu dy^\nu + dy^\mu dx^\nu] \right\} \\ &+ I \left\{ g^A_{\mu\nu}[dx^\mu dx^\nu + dy^\mu dy^\nu] + g^S_{\mu\nu}[dx^\mu dy^\nu + dy^\mu dx^\nu] \right\} \end{aligned} \tag{4}$$

A constraint for the variation of the action S is deduced requiring that the infinitesimal length $d\omega^2$ is real, i.e., that the pseudo-imaginary part is zero, consistent with the assumption that the path of a particle is a geodestic along real distances. This leads to

Einstein equations which have on the right hand side the components of an energy-momentum tensor [15]. The problem is simplified, assuming that in each zero-divisor component the metric is the same, or $g^{+}_{\mu\nu}(X^{+}) = g_{\mu\nu}(x)$ and $g^{-}_{\mu\nu}(X^{-}) = g_{\mu\nu}(x)$. With this assumption the antisymmetric metric combination $g^{A}_{\mu\nu} = 0$ and the length element reduces to

$$d\omega^2 = g_{\mu\nu}[dx^{\mu}dx^{\nu} + dy^{\mu}dy^{\nu}] + 2Ig_{\mu\nu}dx^{\mu}dx^{\nu} \tag{5}$$

where the first term is exactly the one proposed in [14] and also used for the study of a minimal length in [16], whose approach will be followed by us, too. As shown in [15] the constraint $g_{\mu\nu}dx^{\mu}dx^{\nu} = 0$ delivers a solution for y^{μ} , which is

$$y^{\mu} = l\frac{Dx^{\mu}}{D\tau} = l\left(\frac{dx^{\mu}}{d\tau} - \Gamma^{\mu}_{\varrho\xi}\frac{dx^{\varrho}}{d\tau}x^{\xi}\right) \quad , \tag{6}$$

where D is the covariant derivative and τ the eigentime [17]. The derivation of Eq. (6) can be found in [17], page 95f.

The l has the dimension of a distance and is introduced due to dimensional reasons (the coordinate has dimension of length). In pcGR it is treated as a parameter, but here for convenience we assume that it is the Planck length.

For a Minkowski metric $g_{\mu\nu} = \eta_{\mu\nu}$ Eq. (6) just reduces to $y^{\mu} = l\frac{dx^{\mu}}{d\tau}$, the commom ansatz in theories with a maximal acceleration.

3 The pseudo-complex (pc) metric

In what follows, we will split the discussion into two cases: The first case is the Schwarzschild solution, for a non-rotating black hole, where we can illustrate the main structure and effects of the pcGR. The second case is the Kerr solution, which corresponds to a rotating black hole, where new effects will be discussed. For the case of a rotating black hole, we define the angular momentum L in units of mass, i.e., $\lambda = \frac{L}{m}$. For the case of a non-rotating black hole, the one also studied here, we restrict to angular momentum $L = 0$, which implies $\lambda = 0$. This also modifies the equation of motion for the mass times ϕ: $m\ddot{\phi} = -\frac{2\lambda}{y^3}\dot{y}$, which for $\lambda = 0$ is just 0.

In a first step, we will describe the form of the general length element, where a minimal length is included and list the metric for the Kerr case. The Schwarzschild metric is simply obtained by setting the rotational parameter, a, to zero.

The influence of the dark energy is parametrized via the parameter $B_n = bm^n$ [18, 19], which enters the components of the metric, listed below and can also be found in [11]. The influence of the minimal length is obtained by extracting in (5) the expression $ds^2 = d\tau^2 = g_{\mu\nu}dx^{\mu}dx^{\nu}$ ($d\tau$ as the eigen-time), in line with [16]. This straight forward factorization of the eigentime squared, however, comes with a downside: As noted in [16] the direct extraction of ds^2 leads to the following problem: "the effective theory presented is intrinsically non-covariant. Non-covariant is the quadri-acceleration that appears in σ^2 and non-covariant is σ^2 itself which is not, therefore, a true scalar." The problem is related to use the simple derivative and not the covariant derivative of the

velocity and acceleration. Corrections according to Eq. (6) are in order but comlicate the treatment. Therefore, due to simplicity we also use it as an approximation in order to study the effects of a minimal length.

According to [16] (see also [11]), the line element of the pcGR, including a minimal length, can be written as (Note, that the condition $y^\mu = \frac{dx^\mu}{d\tau}$ is used here, which leads to a real length element squared, though this condition is not the general solution as given in (6).)

$$dw^2 = \mathcal{G}_{\mu\nu} dx^\mu dx^\nu = \left(1 - l^2 \left| g_{\varrho\xi} a^\varrho a^\xi \right|\right) g_{\mu\nu} dx^\mu dx^\nu \quad , \tag{7}$$

where a^μ are the acceleration components and $\mathcal{G}_{\mu\nu}$, is the new metric

$$\mathcal{G}_{\mu\nu} = \left(1 - l^2 \left| g_{\varrho\xi} a^\varrho a^\xi \right|\right) g_{\mu\nu} \; = \; \sigma^2 (r)\, g_{\mu\nu} \quad . \tag{8}$$

The $a^\mu = \frac{du^\mu}{d\tau}$ is the acceleration component with τ as the eigentime. It is clear that the conformal factor $\sigma^2 (x^\mu, a^\mu)$ depends on the coordinates x^μ, the components of accelerations a^μ and also a minimal length l that plays an important role in the discussion on the structure of black holes.

The non-zero metric components, $\mathcal{G}_{\mu\nu}$ of the general Kerr solution within pcGR are given by [20, 21]

$$\begin{aligned}
\mathcal{G}_{00} = \sigma^2 (r)\, g_{00} &= \sigma^2 (r)\, \frac{r^2 - 2m_r + a^2 \cos^2\theta + \frac{B_n}{(n-1)(n-2) r^{n-2}}}{r^2 + a^2 \cos^2\theta} \\
\mathcal{G}_{11} = \sigma^2 (r)\, g_{11} &= -\sigma^2 (r)\, \frac{r^2 + a^2 \cos^2\theta}{r^2 - 2mr + a^2 \cos^2\theta + \frac{B_n}{(n-1)(n-2) r^{n-2}}} \\
\mathcal{G}_{22} = \sigma^2 (r)\, g_{22} &= -\sigma^2 (r)\, (r^2 + a^2 \cos^2\theta) \\
\mathcal{G}_{33} = \sigma^2 (r)\, g_{33} &= -\sigma^2 (r) \left(\left(r^2 + a^2\right) \sin^2\theta + \frac{a^2 \sin^4\theta \left(2mr - \frac{B_n}{(n-1)(n-2) r^{n-2}}\right)}{r^2 + a^2 \cos^2\theta} \right) \\
\mathcal{G}_{03} = \sigma^2 (r)\, g_{03} &= 2\sigma^2 (r)\, \frac{-a^2 2mr \sin^2\theta + a \frac{B_n}{(n-1)(n-2) r^{n-2}} \sin^2\theta}{r^2 + a^2 \cos^2\theta}
\end{aligned} \tag{9}$$

The n parametrizes the fall-off of the dark energy density outside a black hole and is, thus, of phenomenological nature. The effects of this parameter is discussed in [11] and shown that the changes, though continuous, are systematic without altering the quality of the result. As we saw in [22, 23] the $n = 2, 3$ are excluded: The $n = 2$ is excluded by solar system experiment and also $n = 3$ is excluded from the first observation of gravitational waves [23]. Thus, we choose $n = 4$ (for larger n the characteristics will not change much). The proposition that there is an accumulation of dark energy, increasing towards the center, is based on [24], where the presence of vacuum fluctuations was deduced in a curved space (see also [8]).

The a in Eq. (9) is the spin parameter with the mass unit m, the mass value observed at infinite distance. For $a = 0$, the metric (9) describes the limiting static and spherically symmetric pc-Schwarzschild geometry with a minimal length.

3.1 pc-Schwarzschild, $a = 0$

For $a = 0$, the line element of pc-Schwarzschild solution is given by

$$dw^2 = \sigma^2(r)\left[\left(1 - \frac{2m}{r} + \frac{B_4}{6r^4}\right)dt^2 - \frac{dr^2}{\left(1 - \frac{2m}{r} + \frac{B_4}{6r^4}\right)} - r^2\left(d\theta^2 + \sin^2\theta\left(d\varphi^2\right)\right)\right] \tag{10}$$

In order to simplify the discussion, from here on we use the following scale parameters

$$y = \frac{r}{m}\ ,\ \tilde{a} = \frac{a}{m}\ ,\ \epsilon = \frac{l}{m}\ ,\ b = \frac{B_4}{m^4}\quad , \tag{11}$$

where y is the scale for the distance and $\tilde{a}$ the scale for the rotation, used in the Kerr section. The ϵ is a measure of the mass relative to the minimal length, corresponding to the Planck mass, i.e., the smaller ϵ, the larger the mass. The b scales the intensity of the dark energy.

The factor $\sigma^2(r)$ is expressed, as shown above, in terms of the acceleration component $a^\mu a_\mu$. This factor is a function of the rescaled radial distance variable y and energy parameter E, the parameter for the accumulation of the dark energy b and a scale parameter for the mass ϵ. The ϵ parameter starts with 1 for a black hole of Planck mass ($m = l$) and lowers continuously when the mass is increased. We also restrict to the motion in the plane with $\theta = \frac{\pi}{2}$.

The factor σ^2 is of the form

$$\sigma^2(y) = \left\{1 - \epsilon^2\left|-\left(1 - \frac{2}{y} + \frac{b}{6y^4}\right)\ddot{t}^2 + \frac{1}{\left(1 - \frac{2}{y} + \frac{b}{6y^4}\right)}\ddot{r}^2 + y^2\ddot{\phi}^2\right|\right\} \tag{12}$$

where

$$\begin{aligned}
\ddot{t} &= \frac{-E}{\left(1 - \frac{2}{y} + \frac{b}{6y^4}\right)^2}\left(\frac{2}{y^2} - \frac{2b}{3y^5}\right)\dot{r} \\
\ddot{r} &= \left(-\frac{1}{y^2} + \frac{b}{3y^5}\right) \\
\ddot{\phi} &= 0 \\
\dot{r}^2 &= \left[E^2 - \left(1 - \frac{2}{y} + \frac{b}{6y^4}\right)\right]
\end{aligned} \tag{13}$$

The length element can be written now as $dw^2 = \sigma^2 ds^2$, with $ds^2 = g_{\mu\nu}dx^\mu dx^\nu$. The modified metric thus is $\mathcal{G}_{\mu\nu} = \sigma^2 g_{\mu\nu}$.

3.1.1 Event Horizons

In order to study the effect of a minimal length on the event horizon, it is necessary to determine the position of the event horizons, where the new metric satisfies $\mathcal{G}_{\mu\nu} = 0$. Of practical importance is only the outer event horizon, because all lower ones are inaccessible. Nevertheless, we will discuss them, too.

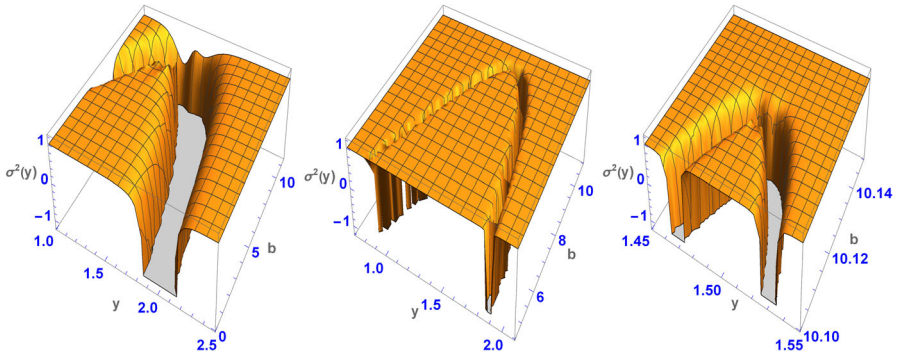

Fig. 1 The factor $\sigma^2(y)$ as a function of y and b. The left figure is for $\epsilon = 10^{-2}$, the central one for $\epsilon = 10^{-4}$ and the right one for $\epsilon = 10^{-6}$

The event horizons can be found by the condition

$$\mathcal{G}_{00} = \sigma^2(r) g_{00}(r_h) = 0 \rightarrow \sigma^2(y_h) = 0 \text{ or } (1 - \frac{2}{y_h} + \frac{b}{6y_h^4}) = 0 \tag{14}$$

By plotting $\sigma^2(y) g_{00}$ as a function in y alone, one can read off the intersections with the y-axis and determine numerically the position of horizons. The second condition has only solutions for $b \leq \frac{81}{8}$.

The event horizons deduced by the condition $\mathcal{G}_{00} = 0$ includes automatically the event horizons for the pc-Schwarzschild solution without a minimal length. Therefore, it is of interest to study the structure of g_{00} and σ^2 separately, only to combine them at the end. In what follows we will first plot the σ^2-function, posterior the g_{00} function and finally the $\mathcal{G}_{00}$. In all examples studied, we will use the common energy scale $E = 1$, while using other scales do not change the structure of the results.

In Figure 1 the $\sigma^2(y)$ factor is plotted as a function in b. The left figure is for $\epsilon = 10^{-2}$, the central figure for $\epsilon = 10^{-4}$ and the right figure for $\epsilon = 10^{-6}$, i.e., for 100, 10000 and a million times the Planck mass. There is a parabolic like structure (see discussion further below), where the maximum coincides with the value of b from which on no event horizon exists, i.e., the observed distinct structure of a deep valley is related to the appearance of an event horizon. In Fig. 1 we note that for decreasing ϵ (increasing mass of the black hole) the valley gets increasingly narrower, which gives evidence that for a macroscopic black hole it will resemble a sheet. This is emphasized in Fig. 2, where epsilon decreased to 10^{-9} and 10^{-10}, i.e., 10^9 and 10^{10} times the Planck mass, the last value corresponding to a black hole mass of approximately $200kg$! The valley structure is clearly visible for these small masses, but it will be less and less visible for increasing masses. For macroscopic black hole the valey is still there but impossible to see in a graph.

The Component g_{00}:

In Fig. 3 the g_{00} component is plotted versus y and b. No special structure is observed, only that from $b = \frac{81}{8}$ downward the g_{00} has a range where it is negative and also an event horizons appears. Fig. 3 also shows in addition the effect of dark energy parameter b on the the event horizon, with the following remarks on three observed cases: In the first case $b = 8 < 81/8$, there are two event horizons y_-, y_+ such that $y_- < \frac{3}{2} < y_+$. In the second case $b = 81/8$, there is a single event horizon at $y_h = 3/2$. Notably, this case is important because the derivative

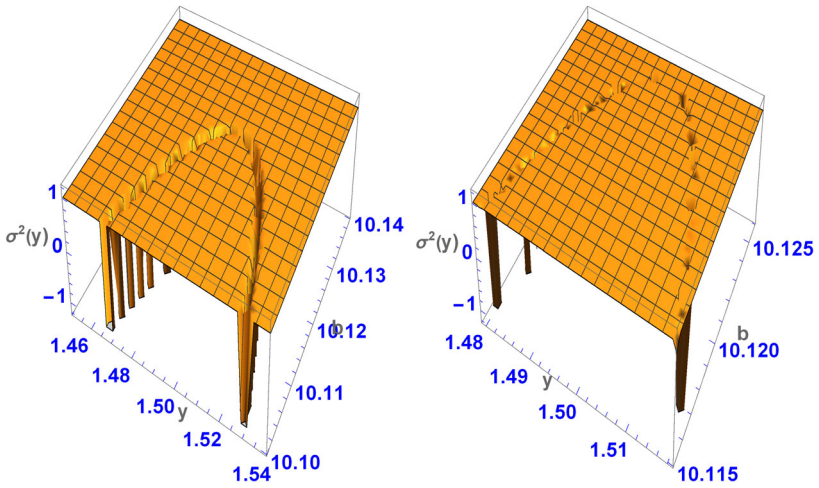

Fig. 2 The factor $\sigma^2(y)$ as a function of y and b, Schwarzschild case. In the left figure $\epsilon = 10^{-9}$ and in the right one it is 10^{-10}

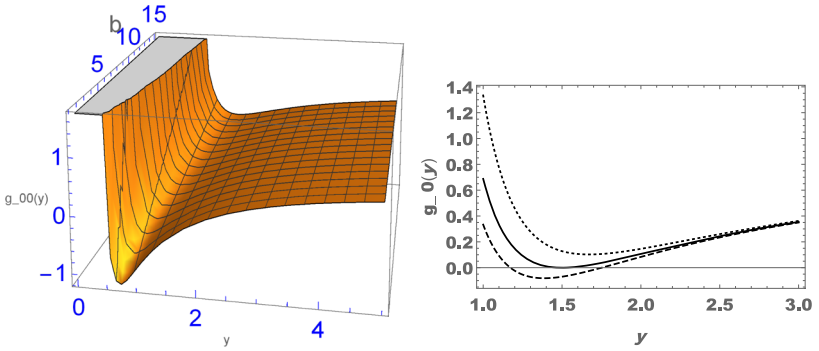

Fig. 3 On the left g_{00} is plotted as a function in y and b. On the right hand figure some cuts for a given b are shown. The solid line corresponds to $b = \frac{81}{8}$, dashed line to $b = 8$ and the dotted line to $b = 14$

of the component g_{00} is also zero, indicating that at $y_h = 3/2$ corresponds to a minimum of g_{00}.

The Component $\mathcal{G}_{00}$

Now, we will examine the combined effects of dark energy b and the minimal length l on the component $\mathcal{G}_{00}$, particularly near the event horizons

As we mentioned above, when g_{00} becomes negative, the plots will exhibit inversions with respect to $\sigma^2(y)$. With that, the plots of $\mathcal{G}_{00}$ will show a more involved structure which, however, can be disentangled by knowing the structure of g_{00} and $\sigma^2(y)$ separately. The information on the influence of a minimal length is contained only in the $\sigma^2(y)$ factor of $\mathcal{G}_{00}$. In Fig. 4 the $\mathcal{G}_{00}$ is shown as a function in b and y. It has a similar structure as $\sigma^2(y)$, save that the inner wall of the parabolic valley goes to $+\infty$ instead of $-\infty$. This is because for $b = 8$ in the region between the two event horizons the g_{00} is negative, thus inverting the corresponding figure of σ^2. Because the g_{00} does not exhibit any chaotic behavior, all the rapid changes in $\mathcal{G}_{00}$ are due to the σ^2-function.

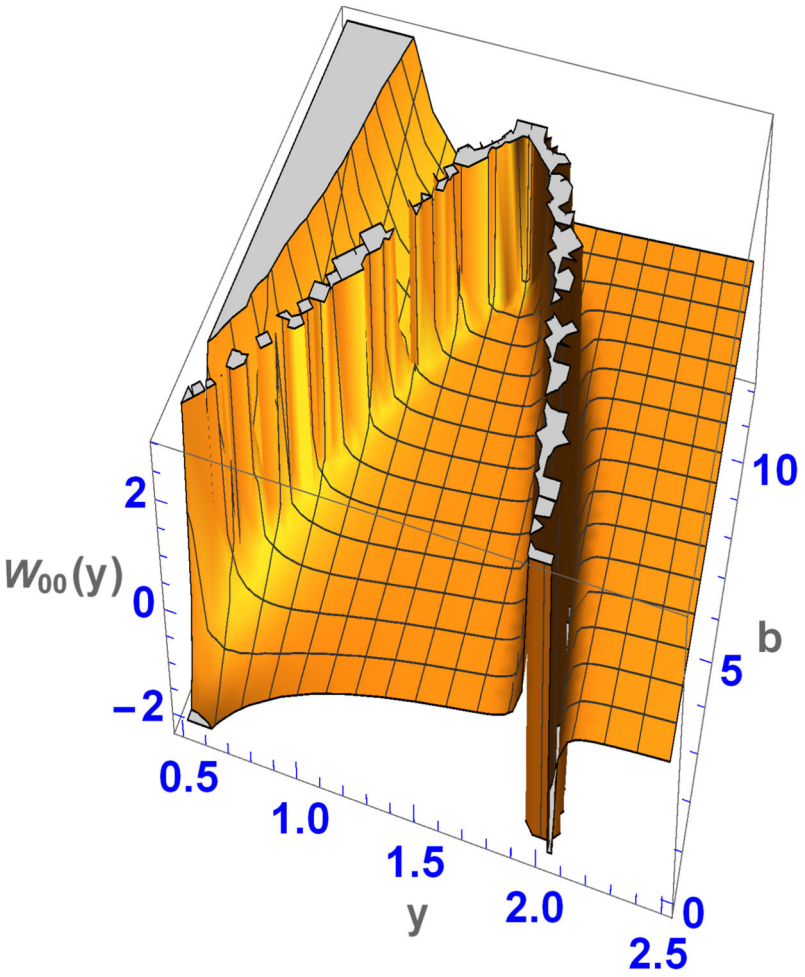

Fig. 4 The Component $\mathcal{G}_{00}(y)$ as a function of y and b, for $\epsilon = l/m = 0.01$. (The "wiggles" in the figure are due to numerical/graphical errors)

The outer wall is going to $-\infty$, which will result in a negative temperature and a negative pressure, as will be discussed in the section of the Hawking temperature.

In Fig. 5 and Fig. 6 some cuts of the $\mathcal{G}_{00}$ as a function in y are presented, in Fig. 5 for $b = 8$ and in Fig. 6 for $b = \frac{81}{8}$. The curves correspond to different values of ϵ. Again we observe that the valley becomes narrower when ϵ decreases (increasing mass). There are several brusk changes at lower positions than the most outer event horizon. They are, thus, of no consequential importance but rather of academic interest.

In conclusion, a valley of infinite depth is building up at the event horizon. This structure disappears when b is large enough to avoid the forming of an event horizon.

The structure of the barriers and their position is now more involved: There are barriers arising from the factor $\sigma^2(y) = 0$, indicating that the effect of minimal length acts as a barrier near the event horizon only for $b < 81/8$. This results in the appearance of additional event horizons is due to the influence of minimal length introduced by $\sigma^2(y)$.

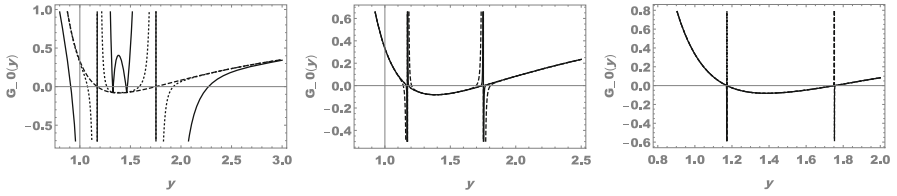

Fig. 5 The component $\mathcal{G}_{00}(y) = \sigma^2(y)g_{00}$ as a function of y for $b = 8$, Schwarzschild case, for different value of ϵ. In the left figure the dashed line is for $\epsilon = 0$ (no minimal length), the solid line for $\epsilon = 0.1$ and the dotted line is for $\epsilon = 0.01$. In the central figure the dashed line corresponds to $\epsilon = 10^{-3}$, the solid line to $\epsilon = 10^{-4}$ and the dotted line to $\epsilon = 10^{-5}$. In the right figure the dashed line corresponds to $\epsilon = 10^{-5}$, the solid line to 10^{-6} and the dotted line to $\epsilon = 10^{-7}$

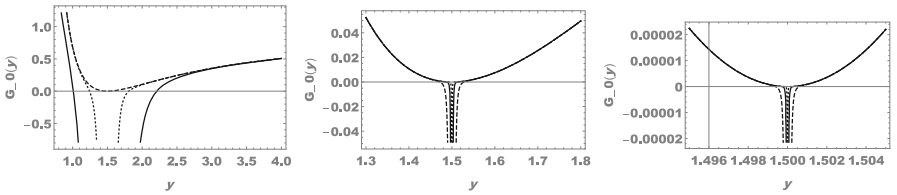

Fig. 6 The component $\mathcal{G}_{00}(y) = \sigma^2(y)g_{00}$ as a function of y and $b = 81/8$, for different value of ϵ. In the left figure the dashed line corresponds to $\epsilon = 0$ (no minimal length), the solid line to $\epsilon = 0.1$ and the dotted line ot $\epsilon = 0.01$. In the central figure the dashed line corresponds to $\epsilon = 10^{-5}$, the solid line to $\epsilon = 10^{-6}$ and the dotted line to $\epsilon = 10^{-7}$. In the right figure, the dashed line is for $\epsilon = 10^{-10}$, the solid line for $\epsilon = 10^{-11}$ and the dotted line to $\epsilon = 10^{-12}$

Figs 5 and 6 illustrate the different possible cases:

- 1. One horizon for $b = 0$ at $y_h = 2$, this corresponds to the GR.
- 2. In Fig. 5 four distinct horizons for $b = 8$ (dashed curve), there are two horizons y_{-1} and y_{-2} near y_- and two horizons y_{+1} and y_{+2} near y_+. For the case $E = 1$ and $l = 10^{-2}$, the values are $y_{-1} = 1.21651$, $y_{-2} = 1.1234$, $y_{+1} = 1.68515$ and $y_{+2} = 1.81903$ with $y_{-1} < y_- < y_{-2}$ and $y_{+1} < y_+ < y_{+2}$;
- 3. In Fig. 6, left panel there appear two horizons near $y_h = 3/2$, for $b = 81/8$, (Solid curve). For example, for $\epsilon = 10^{-2}$ and $E = 1$, we find two events horizons near $y_h = 3/2$, $y_{-h} = 1.35532$, $y_{+h} = 1.64506$, $(y_{-h} < y_h < y_{+h})$. This corresponds to an extremal black hole, because when b is infinitesimal larger, there is no black hole anymore.
- 4. No horizons for $b > 81/8$ for $y > 3/2$;

For $0 < b < \frac{81}{8}$ we have a geometry with non-coincident inner r_{-1}, r_{-2} and outer r_{+1}, r_{+2} horizons. For $b > \frac{81}{8}$ the effects of the minimal length are not dominant.

3.1.2 Hawking Temperature of pc-Schwarzschild

We will determine the Hawking temperature within the pseudo-complex Schwarzschild curvature to analyze the effect of a minimal length for $\epsilon = l/m << 1$. Using [25, 26], we define function $\kappa(y)$, which for $y = y_h$ corresponds to the surface gravity. However, we choose y as arbitrary under the assumption that even outside the black hole, when gravitation is still strong, pairs of particles can be produced, which is in line with [32].

$$\kappa = \frac{1}{2}\frac{\partial \mathcal{G}_{00}}{\partial r} = \frac{1}{2m}\frac{\partial \mathcal{G}_{00}(y)}{\partial y} \quad , \tag{15}$$

The Hawking temperature for arbitrary y is given by

$$T(y) = \frac{\kappa}{2\pi} = (\frac{\sigma^2(y)}{2\pi m y^2})(1 - \frac{b}{3y^3}) \tag{16}$$

It is clear that the difference between the cases with and without a minimal length in the pc-Schwarzschild metric is the presence of the factor $\sigma^2(y)$. This factor will be responsible for the appearance of negative Temperatures. Before doing so, the meaning and consequences of a negative Temperature will be discussed, which are not so uncommon in physical systems:

Normally, in a system where the energy is open to large, infinite energy values, the temperature can only increase, the reason why in atomic systems the temperature increases toward larger excitation. This is different for finite systems, as for example a two-level system [27]. When the lowest level is less than half filled, the temperature is increasing, reaching ∞ when the upper and lower level are half filled. When the excitation proceeds, the temperature jumps from $+\infty$ to $-\infty$ and approaching 0 from the negative side for all particles excited to the upper level. This example includes the physics of lasers and negative temperature are, thus, formally possible. Note, however, that a negative temperature corresponds to a higher excitation and is interpreted as being "hotter" than a positive temperature [28–31]. Because negative temperature states are hotter than any positive-temperature state in thermal contact, heat would flow from the negative-temperature system to the positive-temperature system. The consequence for the entropy ($\frac{1}{T} = \frac{\partial S}{\partial E}$ within a canonical ensemble), as a function of temperature, is as follows: The entropy starts at zero, when only the non-degenerate ground state is occupied, and has a positive slope ($T > 0$), rises to a maximum when the lower and upper levels are half filled and then, with a negative slope due to a negative T lowers again until the maximal excitation is reached, i.e., when the upper level is completely filled and only one microstate is possible. At the maximum of the entropy the temperature jumps from $+\infty$ to $-\infty$. In other words, the minimal length in pcGR not only reflects the quantum-gravitational discreteness of spacetime but also plays a key role in producing the unusual thermodynamic behavior—such as negative temperatures, that arises when the energy is saturated.

This is not the only example. In [28–31] classical spin systems where considered, as ultracold atoms in an optical lattice. In these publications a possible simulation of a black hole in terms of these finite spin system is discussed: As a consequence the authors encountered negative temperatures, resulting in negative pressures, also its thermodynamical origin, which is: The requirement that $\frac{\partial S}{\partial V} = \frac{p}{T} > 0$ leads to the conclusion that when T is negative, also the pressure is negative. The authors of [28, 29] obtained in this manner atomic system which are stable under collapse, as in a simulated black hole. This begs the question, if black holes correspond also to a finite system of elementary building blacks as spins. For more detailed information, please consult the original references.

Transferring it to real black holes, the consequence is that a negative pressure can delay the collapse, or avoid it at all, if T is $-\infty$, with a pressure of $-\infty$ acting against the collapse.

Figure 7 shows the effect of the minimal length for different values of $\epsilon = l/m = 10^{-3}$ and $\epsilon = l/m = 10^{-5}$ and $b = \frac{81}{8}$, which manifests as a divergence of the Hawking temperature to $-\infty$ within the horizon interval $]3/2, 2]$ as b varies. The infinite positive temperature seen in the right figure near $y = 0$ can be explained as follows: For the case $b < 81/8$, we have two event horizons, an outer one at y_+ and an inner one at y_-. At y_+ the Hawking temperature is always negative. At y_- the Hawking temperature is proportional to the factor σ^2, which is negative around y_- approaching infinity, multiplied with the derivative of g_{00} in y, whose sign is negative near y_-. Both lead to a positive value for the temperature, tending to infinity, producing the spike seen. As seen, the influence of the minimal length becomes significant near the event horizon.

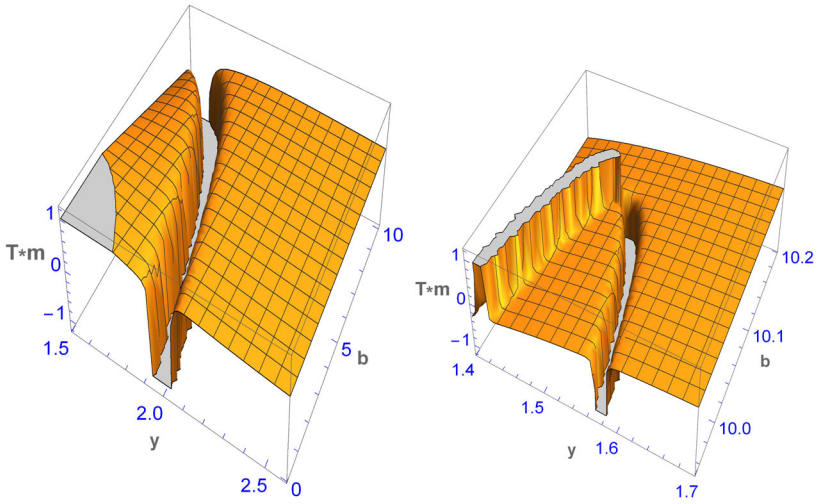

Fig. 7 The Hawking Temperature times mass of the pc-Schwarzschild metric as a function of y and b for different value of ϵ. In the left figure $\epsilon = 10^{-3}$ and in the right figure $\epsilon = 10^{-5}$

Note, that the cut at $b = 0$ in the left figure describes a curve which increases in value, starting from the event horizon, where $T\,m = 0$, to larger y values. It reaches a maximum from which it decreases again. We calculated the Hawking radiation also outside the event horizon, with the assumption, also made in [32], taking into account that pair creation is possible as soon as there is a strong gravitational field, which is called the gravitational Schwinger effect [32].

This is just the behavior encountered in a microscopic derivation of the Hawking temperature [32]. This reassures that our phenomenological approach, easier to apply, is able to reproduce fundamental aspects of the BH and the Hawking temperature.

3.2 pc-Kerr: $a > 0$

In this subsection we will only report on the characteristic changes between the Schwarzschild and Kerr solution.

The pc-Kerr metric corresponds to $a > 0$, using the Boyer-Lindquist coordinates and its pseudo-complex equivalent. The line element is given by

$$\begin{aligned} dw^2 = \sigma^2(r)\Bigg[&-\left(1-\frac{\Psi}{\Sigma}\right)dt^2 + \frac{\Sigma}{\Delta}dr^2 + \Sigma d\theta^2 \\ &+\left(\left(r^2+a^2\right)+\frac{a^2\Psi}{\Sigma}\sin^2\theta\right) \\ &\sin^2\theta d\phi^2 - 2a\frac{\Psi}{\Sigma}\sin^2\theta\,(dtd\phi)\Bigg] \quad . \end{aligned} \tag{17}$$

We will restrict to $E = 1$, in order to define an energy scale, as already mentioned further above. We also recall that the angular momentum per mass is defined as $\lambda = \frac{L}{m}$ and assuming that $L = 0$ also the $\lambda = 0$.

The Boyer-Lindquist coordinates are defined by

$$\Psi(y) = 2y - \frac{b}{6y^2}\ ,\ \Sigma(y)\ =\ y^2 + \tilde{a}^2\cos^2\theta\ ,\ \Delta(y)\ =\ y^2 - 2y + \tilde{a}^2\quad . \tag{18}$$

In what follows, we will consider only motions in the orbital plane with $\theta = 0$.

The factor $\sigma^2(y)$, in terms of the parameters y , $\lambda, \widetilde{a}, b$ and ϵ, is given by

$$\sigma^2(y) = 1 - \epsilon^2\left[\left(1 - \frac{\Psi(y)}{y^2}\right)\left(\ddot{t}\right)^2 - \frac{y^2}{\Delta(y)}\left(\ddot{y}\right)^2 - \left(\left(y^2 + \widetilde{a}^2\right) + \frac{\widetilde{a}^2\Psi(y)}{y^2}\right)\left(\ddot{\phi}\right)^2 + \frac{2\widetilde{a}\Psi(y)}{y^2}\left(\ddot{t}\ddot{\phi}\right)\right] \tag{19}$$

and the accelerations are

$$\begin{aligned}
\ddot{t} &= \left[\frac{2E}{\Delta}y - \frac{E\Delta'}{\Delta^2}\left(y^2 + \widetilde{a}^2\right) - \frac{2\widetilde{a}\Psi}{y^3\Delta}(\widetilde{a}E) + \frac{\Psi'\widetilde{a}}{y^2\Delta}(\widetilde{a}E) - \frac{\widetilde{a}\Psi\Delta'}{y^2\Delta^2}(\widetilde{a}E)\right]\dot{y}\\
\ddot{\phi} &= \left[-\frac{\lambda\Delta'}{\Delta^2} + (\widetilde{a}E)\left(\frac{\Psi'}{y^2\Delta} - \frac{2\Psi}{y^3\Delta} - \frac{\Psi\Delta'}{y^2\Delta^2}\right)\right]\dot{y}\\
\ddot{r} &= \left[-\frac{\Delta'}{2y^2} + \frac{\Delta}{y^3} - \frac{1}{r\Delta}\left(2E^2\left(y^2 + \widetilde{a}^2\right)\right) + \left(\frac{\Delta'}{2y^2\Delta} + \frac{1}{\Delta y^3}\right)\left(-E^2\left(y^2 + \widetilde{a}^2\right)^2\right)\right.\\
&\quad + \frac{\Psi'}{2\Delta}\left(-E^2 + \frac{a^2(\widetilde{a}E)^2}{y^4}\right) - \frac{(\widetilde{a}E)^2}{y^4\Delta}\Psi\Psi' + \frac{(\widetilde{a}E)^2}{2y^4\Delta}\left(\frac{\Delta'}{\Delta} + \frac{4}{y}\right)\Psi^2\\
&\quad \left.+\Psi\left(\frac{\Delta'}{2\Delta^2}\left(E^2 + \frac{\widetilde{a}^2(\widetilde{a}E)^2}{y^4}\right) + \frac{2}{\Delta r^3}\left(\frac{\widetilde{a}^2(\widetilde{a}E)^2}{y^2}\right)\right)\right]
\end{aligned} \tag{20}$$

with

$$\begin{aligned}
\Psi' &= \frac{d\Psi}{dy} = 2 + \frac{b}{3y^3}\\
\Delta' &= \frac{d\Delta}{dy} = 2y - \Psi' = 2y - 2 - \frac{b}{3y^3}\\
\dot{y}^2 &= -\frac{\Delta}{y^4}\left[y^2 + (\widetilde{a}E)^2\frac{\Psi^2}{\Delta^2}\right] - \frac{\Psi}{y^4\Delta}\left[E^2y^4 - \widetilde{a}^2(\widetilde{a}E)^2\right]\\
\Psi(y) &= \frac{\Psi(r)}{m^2},\ \text{and}\ \Delta(y) = \frac{\Delta(r)}{m^2}
\end{aligned} \tag{21}$$

Though, the formulas show a more involved structure, it still shares a lot of properties with the Schwarzschild case.

3.2.1 Event Horizons

The event horizons are determined in the same manner as in the Schwarzschild case, save that $\mathcal{G}_{00} = \sigma^2(y)g_{00}$ has changed. Here, we will only take the specific value, namely $\tilde{a} = 0.75$. It is above 0.5, which is the limit from which on an accretion disk can reach the surface of the

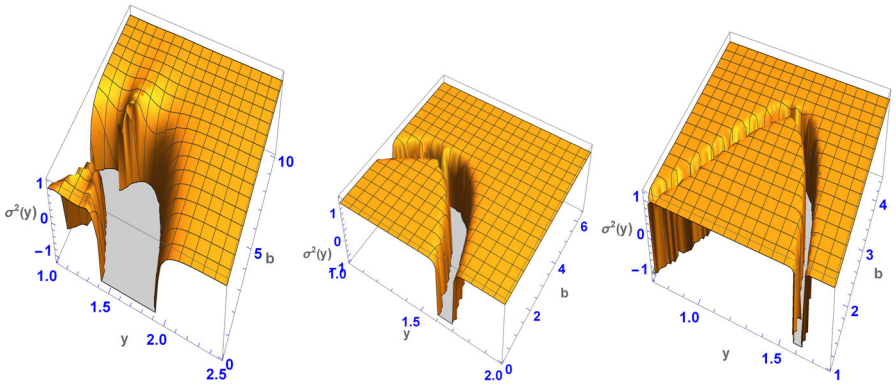

Fig. 8 The factor $\sigma^2(y)$ as a function of y and b, for different values of ϵ and $\tilde{a} = 0.75$. The left figure is for $\epsilon = 0.01$, the central figure for $\epsilon = 10^{-4}$ and the right figure for $\epsilon = 10^{-6}$

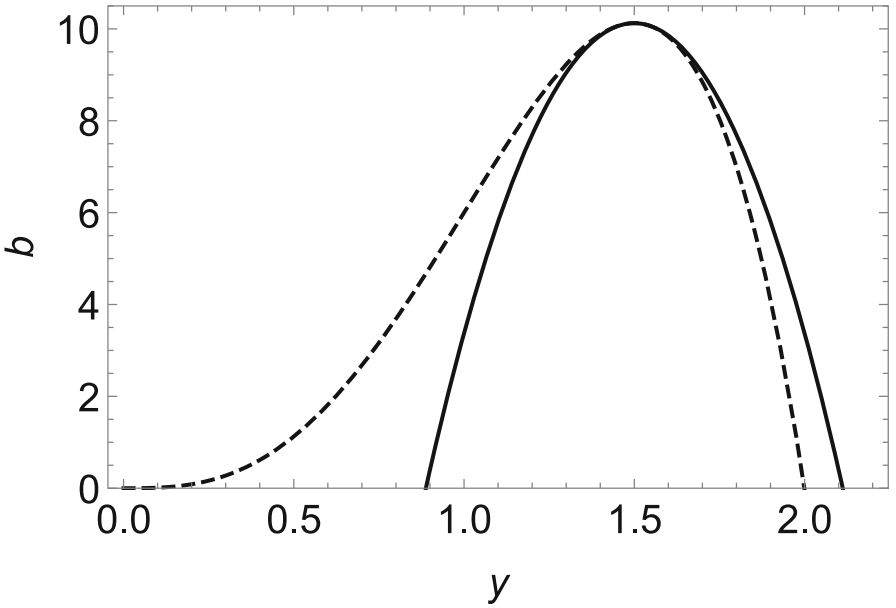

Fig. 9 The dashed line depicts the solution of b as a function in y of the event horizon equation (14), while the solid line corresponds to a parabolic approximation of this solution

star [19] and it is not the maximal value of 1. A systematic study would take too much space and not change the main conclusions. The valley structure reminds at a "'parabola"', though strictly speaking it is not (see discussion further below). In Fig. 8 three cases for ϵ are plotted, which can be compared to Fig. 1. The maximum of this curve is now shifted to lower values of b, a consequence of $\tilde{a} > 0$. Otherwise, the exhibited properties are similar to the Schwarzschild case.

Choosing this representative value of $\tilde{a} = 0.75$, one observes the following: Fig. 8 shows that there is no event horizon above $b > \frac{81}{32}(\frac{1}{\sqrt{2}} + \frac{11}{16})$, unlike the case when $\widetilde{a} = 0$ when there

is no event horizon for values $b > 81/8$. The solution of the limiting value of b is obtained solving the equation for the event horizon as given in Eq. (14), second condition, which can be rewritten into $6y^4 - 12y^3 + b = 0$. This solution can be most easily found using an algebraic routine. The solution of the equation will not be a parabola, though from the figures it looks like it. To illustrate the deviation from a parabolic behavior, we plot in Fig. 9 two curves: The dashed one is the solution of the event horizon equation, rewritten in terms of $b = 6y^3(2 - y)$ and the second curve, a parabola, corresponds to the equation $b = 81/8 - 27(y - \frac{3}{2})^2$. While around the maximum the agreement is fine, for lower values of y a clear deviation from the parabolic behavior is seen. This indicates that the limiting value, from which on no event horizon exists, decreases as the parameter $\widetilde{a}$ increases. This relation between $\widetilde{a}$ and b does not depend on the minimal length.

The difference between pc-Schwarzschild and pc-Kerr is that the factor $\sigma^2(y)$ diverges at $y = \frac{3}{4}(1 + \frac{1}{\sqrt{2}})$ when $b = \frac{81}{32}(\frac{1}{\sqrt{2}} + \frac{11}{16})$ for $\widetilde{a} = 0.75$, whereas the factor $\sigma^2(y)$ approaches 1 toward $y = \frac{3}{2}$ when $b = 81/8$ for $\widetilde{a} = 0.75$.

We note here, that the value $b = \frac{81}{32}(\frac{1}{\sqrt{2}} + \frac{11}{16})$ represents the minimal value where $g_{00} = 0$ at $y = \frac{3}{4}(1 + \frac{1}{\sqrt{2}})$ for $\widetilde{a} = 0.75$.

This is the main characteristic change between the Schwarzschild and Kerr solution. All other effects observed in the Schwarzschild case also will be seen in the Kerr case. Thus, it is of no use to repeat the results here.

With respect to the Hawking temperature, the formula changes to

$$T = \frac{k}{2\pi} = \frac{\sigma^2(y)}{2\pi m y^2}\left(1 - \frac{a^2\cos^2(\theta)}{y} - \frac{b}{3y^2}\right)\left(1 + \frac{a^2\cos^2(\theta)}{y}\right) \quad . \tag{22}$$

Apart from a distortion due to a, every finding stays qualtitatively the same. The derivation is the same as for the Schwarzschild case. Again, the metric $\mathcal{G}_{00}$ from Eq. (9) is derived with respect to y.

4 Conclusion

We have investigated the effects of a minimal length on a black hole, with an emphasis on small black holes. In order to do so, we applied an effective theory of General Relativity which includes the possible effects of accumulating dark energy, a consequence attributed to vacuum fluctuation in curved space [7, 8]. The effective theory applied is called *pseudo-complex General Relativity* (pcGR) [9–11]. In this theory the dark energy is modeled via a parameter b, which for $b = 0$ corresponds to the standard theory of General Relativity.

The metric was modified such that the standard length element squared (dw^2) acquires a factor, called σ^2, which contains all information of the minimal length. When $l = 0$ the GR is obtained, but for $l \neq 0$ effects become dominant near and below the position of the outer event horizon, which also depends on the amount of dark energy accumulated, modeled by the parameter b. First, the Schwarzschild case was considered and then briefly extended to the Kerr case. In both cases, the effects of the minimal length are characteristically the same.

The main effect is the formation of an infinitely deep valley in the metric at the position of an event horizon. The effect disappears when there is no event horizon. The consequence of this valley is the appearance of a negative temperature, which in turn produces negative pressures, stabilizing the black hole. When the rotational parameter a increases, the basic structure is the

same, save that the limiting $b = \frac{81}{8}$ above which no event horizon exists anymore, shifts to lower values.

Due to the similarity of a black hole to finite spin systems (see [28–30]) and the appearance of negative temperatures which results in a negative, our results add to the suspicion that black holes can be considered as systems of finite building blocks, which may be an important hint to their microscopic structure.

We found that a black hole can not only be stabilized by adding a dark energy, but the presence of a minimal length can do it, too. However, our considerations are made for a static black hole. In order to verify that a collapsing mass, forming a black hole, can be stabilized, a dynamical consideration has to be done, which we will consider in a future work.

Our interpretation is that, due to the potential barriers, combined with the appearance of negative temperatures (implying negative pressures), the formation small (primordial) black holes is suppressed and macroscopic black holes may be stabilized due to the appearance of these pressures and of the minimal length.

Acknowledgements L.M. and P.O.H. acknowledge financial support from DGAPA-PAPIIT (IN116824).

Author Contributions Peter O. Hess: writing original manuscript, investigation, validation and editing L. Maghlaoui: Investigation, validation and editing

Data Availability No datasets were generated or analysed during the current study.

Declarations

Competing interests The authors declare no competing interests.

References

1. Misner, C.W., Thorne, K.S., Wheeler, J.A.: Gravitation, 2nd edn. W.H. Freeman and Company, San Francisco (1971)
2. Smolin, L.: Three Roads to Quantum Gravity (Basic Books,Michigan,1001)
3. Blumenhagen, R., Lüst, D., Theisen, S.: Basic Concepts of String Theory. Springer, München (2013)
4. Buchdahl, H.A.: MNRAS **150**(1), 1–8 (1970)
5. Hořawa, P.: Phys. Rev. D **79**, 084008 (2009)
6. Gimenez, J.G.G., Hadjimichef, D., Hess, P.O., Netz-Marzola, M.: C. A. Zen Vasconcellos Universe **11**, 5 (2025)
7. Visser, M.: Phys. Rev. D **54**, 5116 (1996)
8. Birrell, N.D., Davis, P.C.W.: Quantum Fields is Curves Space. Cambridge University Press, London (1982)
9. Hess, P.O., Greiner, W.: Int. J. Mod. Phys. E **18**, 51 (2009)
10. Hess, P.O., Schäfer, M., Greiner, W.: Pseudo-Complex General Relativity. Springer, Heidelberg (2015)
11. Hess, P.O.: Prog. in Part. and Nucl. Phys. **114**, 103809 (2020)
12. Kelly, P.F., Mann, R.B.: Class. and Quant. Grav. **3**, 705 (1986)
13. Hess, P.O., L'opez-Moreno, E.: AN **342**, 1034 (2021)

14. Caianiello, E.R.: Il Nuovo Cim. Lett. **32**, 65 (1981)
15. Maghlaoui, L., Hess, P. O.: AN **345**, 20230151 (2024)
16. Feoli, A., Lambiase, G., Papini, G., Scarpetta, G.: Phys. Lett. A **268**, 247 (2000)
17. Adler, R., Bazin, M., Schiffer, M.: Introduction to General Ralativity, 2nd edn. Mcgrw-Hill, New York (1975)
18. Hess, P.O., Greiner, W.: Int. J. Mod. Phys. E **18**, 51 (2009)
19. Hess, P.O., Schäfer, M., Greiner, W.: Pseudo-Complex General Relativity. Springer, Heidelberg (2016)
20. Hess, P.O., López-Moreno, E.: Universe **5**, 19 (2019)
21. Schönenbach, T., Caspar, G., Hess, P.O., Boller, T., Müller, A., Schäfer, M., Greiner, W.: MNRAS **442**, 121 (2014)
22. Will, C.M.: Liv. Rev. Relat. **9**, 3 (2006)
23. Nielsen, A., Birnholz, O.: AN **339**, 298 (2018)
24. Visser, M.: Phys. Rev. C **54**, 5136 (1996)
25. Maghlaoui, L., Hess, P.O.: AN **345**, 230171 (2024)
26. Padmanabhan, T.: Phys. Rep. **406**, 49 (2005)
27. Greiner, W., Neise, L., Stoecker, H.: Thermodynamics and Statistical Mechanics. Springer, Heidelberg (1995)
28. Braun, S.: Negative Absolute Temperature and the Dynamics of Quantum Phase Transitions, PhD thesis, Fakultät für Physik der Ludwig-Maximilians-Universität München, Germany (2014)
29. Braun, S., 1, Ronzheimer, J. P., Schreiber, M., Hodgman, S. S., Rom, T., 1, Bloch, I., Schneider, U.: Science **339** (January 4), 52 (2013)
30. Oppenheim, J.: Phys. Rev. E **68**, 016108 (2003)
31. Volovik, G. E.: Negative temperature: further extensions (2021). arXiv:2104.01013 [gr-qc]
32. Wondrak, M.F., van Suijlekom, W.D., Falcke, H.: Phys. Rev. Lett. **130**, 221502 (2023)